frontiers | Frontiers in Earth Science

ORIGINAL RESEARCH
published: 06 June 2022
doi: 10.3389/feart.2022.905642

Experimental Study on Mechanical Properties of Gas Storage Sandstone and Its Damage Under Temperature and Pressure

Xiaoping Wang[1], Lehua Wang[1], Baoyun Zhao[2], Yingjie Wu[2], Jiaosheng Yang[3] and Junchang Sun[3]*

[1]College of Civil Engineering and Architecture, China Three Gorges University, Yichang, China, [2]School of Civil Engineering and Architecture, Chongqing University of Science and Technology, Chongqing, China, [3]Petro China Research Institute of Petroleum Exploration & Development, Beijing, China

With the ever-increasing demand for energy, energy mining is developing in the deep underground. In this paper, a conventional triaxial test and a triaxial test at different temperatures (45 MPa confining pressure) have been carried out for sandstone in Hutubi gas storage, and the mechanical properties of the sandstone at different temperatures are analyzed. Based on the damage theory, the damaged relationship of sandstone under thermal-mechanical coupling is deduced, and the damage evolution law of sandstone in gas storage is analyzed. The results show that: 1) In the conventional triaxial test, as the confining pressure increases, the peak strength and elastic modulus of the sandstone are higher, and the specimen is partially sheared and damaged. 2) In the triaxial test under the effect of temperature, the peak strength of the sample decreases with the increase of temperature. Compared with the four stages of the conventional triaxial test, the stress-strain curve adds a ductility stage. The failure mode of the sample is mainly micro-cracks extended ductile destruction. 3) Under the thermal-mechanical coupling of sandstone, the higher the test temperature, the greater the initial damage of the sample. With the joint action of axial force and temperature, the damage of specimen becomes more obvious. This research results can provide the experimental basis and mechanism understanding for the analysis of mechanical properties of gas storage sandstone and the application of deep underground engineering.

Keywords: sandstone, high temperature, high pressure, strengtch, damage evolution

OPEN ACCESS

Edited by:
Yuan Xu,
University of Oxford, United Kingdom

Reviewed by:
Junbao Wang,
Xi'an University of Architecture and Technology, China
Xiaoping Zhou,
Chongqing University, China

****Correspondence:***
Baoyun Zhao
baoyun666@cqust.edu.cn

Specialty section:
This article was submitted to Structural Geology and Tectonics, a section of the journal Frontiers in Earth Science

Received: *27 March 2022*
Accepted: *05 May 2022*
Published: *06 June 2022*

Citation:
Wang X, Wang L, Zhao B, Wu Y, Yang J and Sun J (2022) Experimental Study on Mechanical Properties of Gas Storage Sandstone and Its Damage Under Temperature and Pressure. Front. Earth Sci. 10:905642. doi: 10.3389/feart.2022.905642

INTRODUCTION

In recent years, with the increasing demand for energy in China, more and more energy projects have entered deep mining. When a rock mass exists deep within the strata, the mechanical properties and deformation properties of rock mass are significantly different from the engineering response of shallow rock mass (Qian, 2007; Xie, 2017). At the same time, the study of mechanical properties and deformation of engineering rock mass in the high ground stress, high ground temperature, and high karst water pressure environment plays an important role in the stability of deep engineering. Therefore, it is necessary to conduct in-depth research on the mechanical properties of rock mass under high confining pressure and high temperature to reveal the failure characteristics of the rock mass.

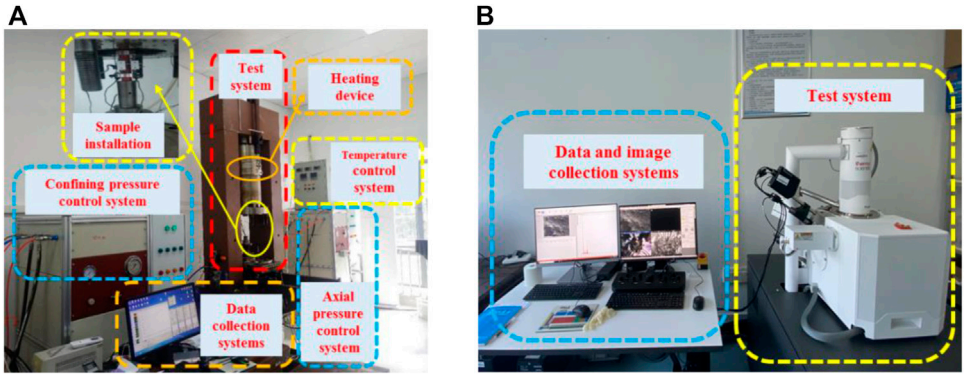

FIGURE 1 | Test equipment. **(A)** The TFD-2000 triaxial test system. **(B)** The Scanning electron microscope.

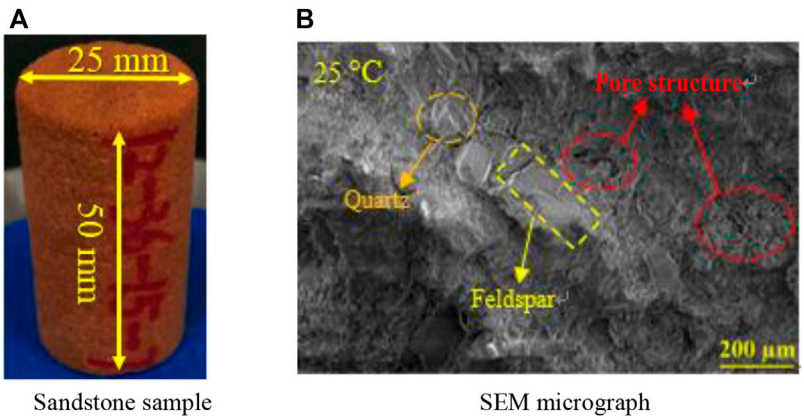

FIGURE 2 | Sandstone sample and SEM micrograph. **(A)** Sandstone sample. **(B)** SEM micrograph.

TABLE 1 | Sandstone test plan for gas storage.

Sample No.	Diameter/mm	Length/mm	Density g/cm^3	Confining pressure/MPa	Temperature/°C
1	25.20	51.00	2.05	0	25
2	25.30	52.00	2.23	10	25
3	25.30	51.20	2.22	20	25
4	25.20	51.10	2.28	30	25
5	25.30	52.30	2.22	45	25
6	24.81	49.84	2.01	45	30
7	25.07	51.00	2.09	45	60
8	25.10	51.00	2.09	45	75
9	25.10	52.00	2.07	45	90

Many scholars have conducted a lot of research on the mechanical properties and deformation characteristics of rock mass under the action of high ground stress, high ground temperature, and high karst water, and some important results have been obtained. Under high ground stress conditions, Corfdir and Sulem (2008) conducted comparative tests of tension and triaxial compression of tight sandstone and sandstone. Beibei Yang et al. (2020) conducted multi-stage cyclic loading and unloading triaxial compression tests on granite and red sandstone under two stress paths with different confining pressures, different amplitudes, and the same amplitude. Zhou (2006) studied the shear failure

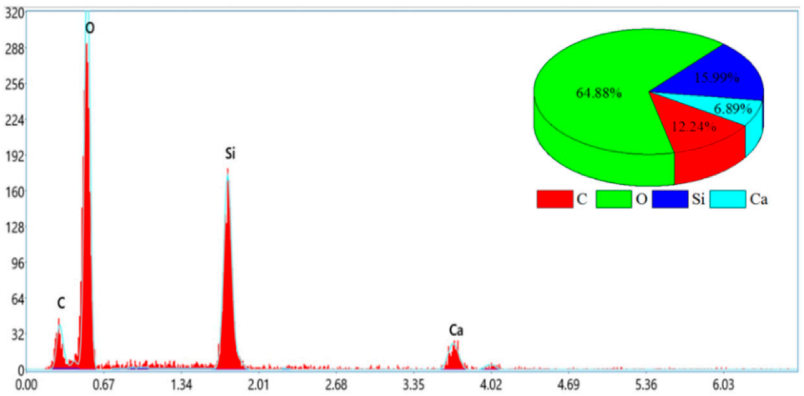

FIGURE 3 | Energy spectrum analysis and mineral element content of sandstone in gas storage.

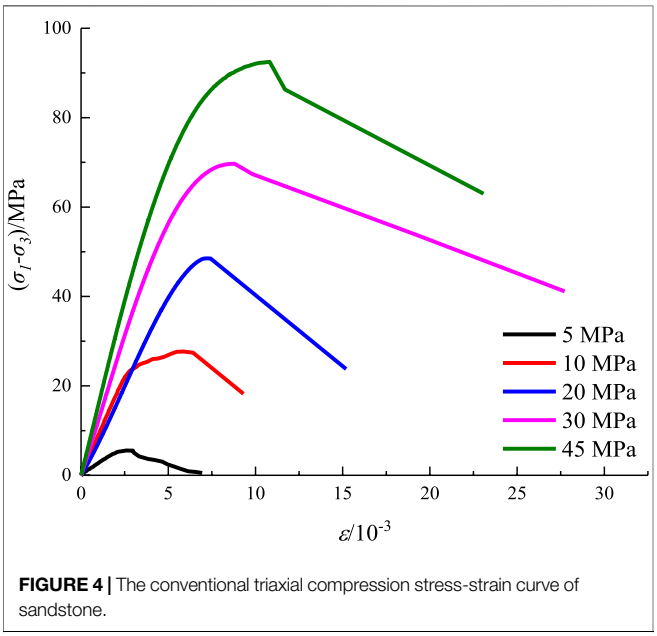

FIGURE 4 | The conventional triaxial compression stress-strain curve of sandstone.

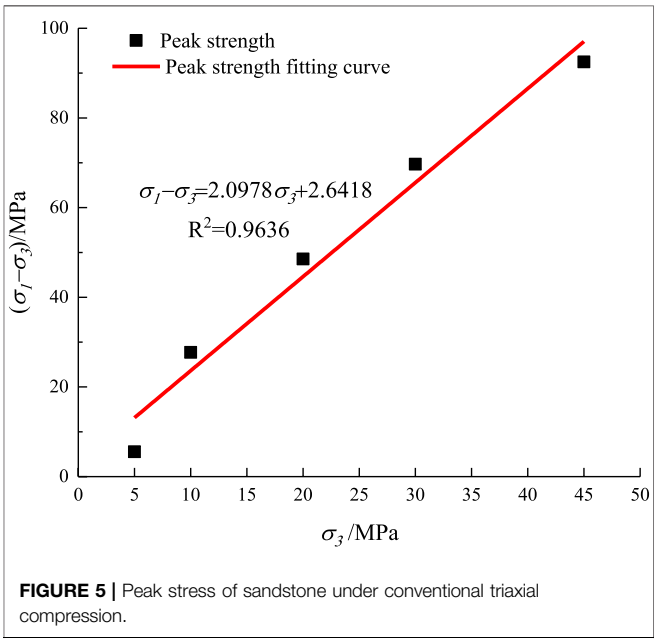

FIGURE 5 | Peak stress of sandstone under conventional triaxial compression.

direction of brittle rock under triaxial compression by using strain energy density factor method. Li and Gong (2020) carried out triaxial single-cycle loading and unloading compression tests of red sandstone samples under different values of confining pressure to study the energy storage characteristics of deep rocks. Chen et al. (2021) studied the mechanical properties of rock-coal composite specimens by triaxial compression tests with confining pressures ranging from 0 to 20 MPa. Taking the temperature effect of the rock into consideration, Zhao et al. (2017) carried out the acoustic emission characteristics and macroscopic mechanical properties evolution of granite under high temperature and high pressure. Kumari et al. (2019) studied the effects of different heating temperatures (from room temperature to 1,000°C) and cooling treatments (constant high temperature, slow cooling, and rapid cooling) on the tensile strength and microstructure changes of Australian granite. Zhou et al. (2021) carried out uniaxial compression tests of granite with prefabricated cracks at three dip angles and thermal-mechanical coupling at 25–700°C, and studied the relationship between strength change of granite specimens and crack arrangement and temperature. Qin et al. (2020) conducted uniaxial and triaxial tests to study the physical and mechanical properties of granite before and after high-temperature treatment at an indoor temperature of 1,000°C. Yin et al. (2021) experiment show that the development of thermal defects increases sandstone porosity from 18.59 to 26.49% in the range of 100–800°C. Tang et al. (2019) studied the effects of temperature and time on the physical, thermoelectric, and mechanical properties of fine marble. Zhang et al. (2019) studied the impact of sandstone micro-damage on macro-physical and mechanical properties under

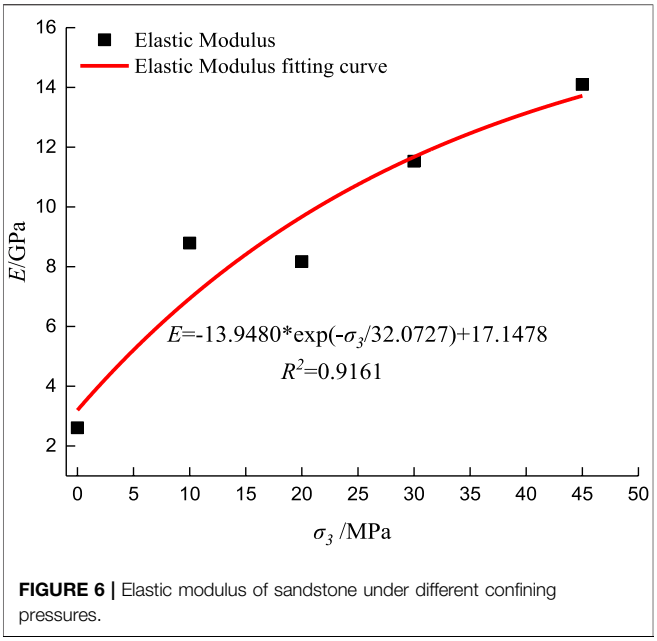

FIGURE 6 | Elastic modulus of sandstone under different confining pressures.

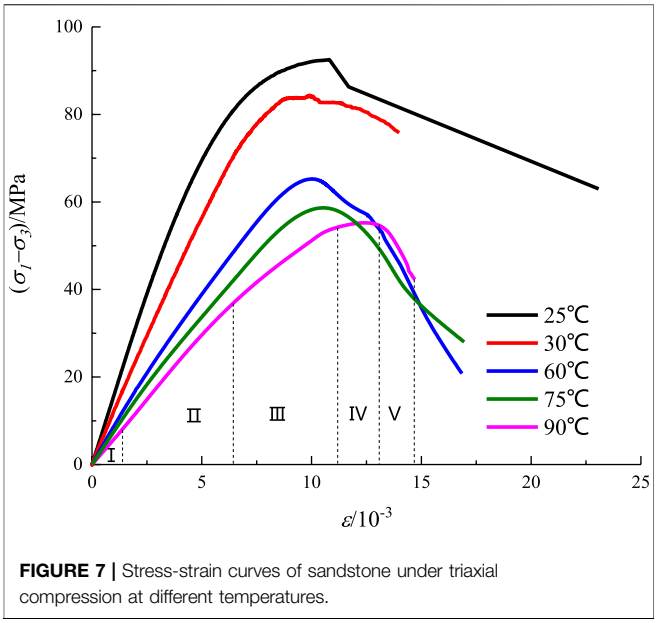

FIGURE 7 | Stress-strain curves of sandstone under triaxial compression at different temperatures.

high temperatures. Mohamadi and Richard (2016) used triaxial compression tests to study the mechanical properties of shale under the coupling effect of high ground stress and high temperature. Wang et al. (2019) and Sheng-Qi Yang et al. (2020) studied the anisotropy of permeability of rock under high temperature, triaxial stress, and thermal crack anisotropy. Taheri et al. (2020) carried out triaxial creep experiments on Gachsaran salt samples under different temperatures and stresses. Meng et al. (2020); Meng et al. (2021) revealed that the stress-strain curve, strength and deformation characteristics, failure mode, and peak stress of rock at high temperature decreased, and the deformation of rock after treatment had elastic aftereffect, and the stress-strain curve formed hysteresis loop. Ma et al. (2020) investigated the effects of temperature and horizontal stress on the mechanical behaviors of granite. In order to study the influence of high-temperature treatment on the mechanical behavior of sandstone under unloading conditions, Xiao et al. (2021) conducted true triaxial unloading tests of σ_1 and σ_3 stress paths on the sandstone samples after heat treatment. Based on the variation of deformation modulus with time in creep process of salt rock, Wang et al. (2020) used deformation modulus to represent elastic modulus of damaged rock material, and established creep damage evolution equation of rock. Zhu et al. (2021) established a thermal damage statistical constitutive model based on the Weibull distribution function combined with the modified Mohr-Coulomb criterion. Wang et al. (2022) conducted fatigue tests on salt rock samples under different maximum cyclic stresses to study the microstructure changes and damage evolution law of salt rock under cyclic loading. Zhou et al. (2020) made rock-like materials with different dip angles, and studied the cracking behavior of rocks with defects after high temperature treatment, indicating that temperature has an important influence on the stress-strain curve and cracking behavior of rock materials with defects.

There are many studies of high confining pressure triaxial compression test on the rock after high-temperature treatment, and relatively few studies have considered the coupling effect of temperature and load at the same time. In fact, the mechanical properties of deep rock masses are the result of the simultaneous coupling of high ground stress and high ground temperature or even high karst water pressure. Therefore, based on previous research ideas, this paper has carried out a comparative study between conventional triaxial compression tests of gas storage sandstone and triaxial compression tests at different temperatures, and aimed to reveal the mechanical properties of sandstone under different confining pressures and temperatures. The constitutive relation under thermo-mechanical coupling was established to characterize the damage degree of sandstone and to analyze the damage evolution process and damage evolution mechanism of sandstone.

TRIAXIAL COMPRESSION TEST

Test Equipment

This test was completed on the TFD-2000 microcomputer servo-controlled rock triaxial test system as shown in **Figure 1A** of Chongqing University of Science and Technology. The test equipment consists of axial loading, confining pressure loading, pore fluid pressure, numerical control, and measurement systems. The maximum axial load is 2000 KN, and the measurement resolution is 10 N. The maximum confining pressure is 80 MPa, and the measurement resolution is 0.001 MPa. The maximum axial deformation is 10 mm, and the measurement accuracy is ± 0.5%. The temperature range is from atmospheric

TABLE 2 | Mechanical parameters such as peak strength of sandstone in triaxial compression.

Sample No.	Temperature *T*/°C	Peak strength/MPa	Elasticity modulus *E*/GPa	Poisson's ratio υ
5	25	92.49	14.10	0.11
6	30	84.35	10.48	0.18
7	60	65.24	6.90	0.29
8	75	58.65	6.06	0.32
9	90	55.25	5.44	0.37

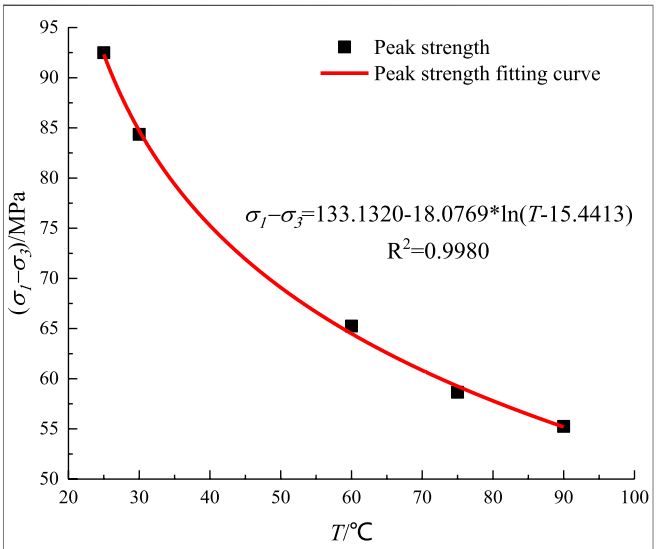

FIGURE 8 | The relationship between temperature and peak strength of sandstone under triaxial compression.

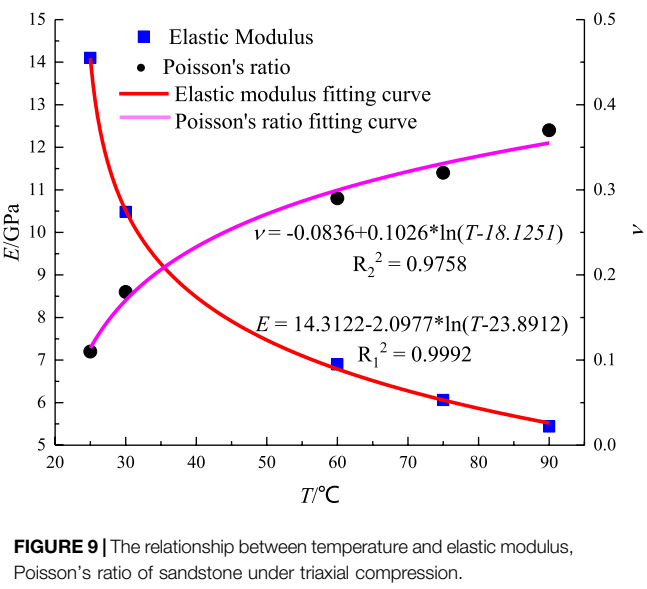

FIGURE 9 | The relationship between temperature and elastic modulus, Poisson's ratio of sandstone under triaxial compression.

temperature to 200°C, and it can directly perform triaxial compression and rheological tests under thermal-mechanical coupling conditions. The equipment can be operated by computer to automatically control test loading and data collection to ensure the safety, timeliness, and accuracy of test analysis.

Test Scheme

This test uses sandstone from the Hutubi gas storage in Changji, China, and the sampling depth is about 3,585 m, which is a sedimentary rock type. In order to simulate the actual storage conditions of the gas storage as much as possible, the sandstone used in this test was prepared into samples with a water content of 2.31%. The sample was processed and polished into a standard cylindrical sample according to the *ISRM* test procedure as shown in **Figure 2A**. The basic physical parameters and test plan of the sandstone used in this test are shown in **Table 1**.

In order to avoid the influence of temperature changes on the test results, the air conditioner is used for indoor temperature control, and the temperature is controlled at 25°C (indoor temperature) during the conventional triaxial test. The oil temperature is added to the test set value (respectively 30°C, 60°C, 75°C, and 90°C) at a speed of 10°C/min and kept at a constant temperature of 2 h so that the sample is evenly heated in the triaxial compression test at different temperatures. At a constant temperature to a predetermined time, confining pressure is loaded at a speed of 0.5 MPa/s, and axial pressure is loaded to hydrostatic pressure at the corresponding rate. Then, an axial load is applied in a load control mode of 0.5 MPa/s until the sandstone loses its bearing capacity.

The scanning electron microscope (as shown in **Figure 1B**) was used to observe the original microstructure of sandstone, as shown in **Figure 2B**. It can be seen from **Figure 2B** that the sandstone particles in this test are loose. According to the test results of energy spectrum analysis, the main elements of the original sandstone samples of the gas storage are O, Si, C and Ca. The content of each element is shown in **Figure 3** combined with the micrograph of **Figure 2B**. The sandstone contains partial quartz and feldspar.

ANALYSIS OF TRIAXIAL COMPRESSION TEST RESULTS

Analysis of Conventional Triaxial Compression Test Results

Figure 4 shows the conventional triaxial compression stress-strain curve of sandstone. It can be seen from **Figure 4** that

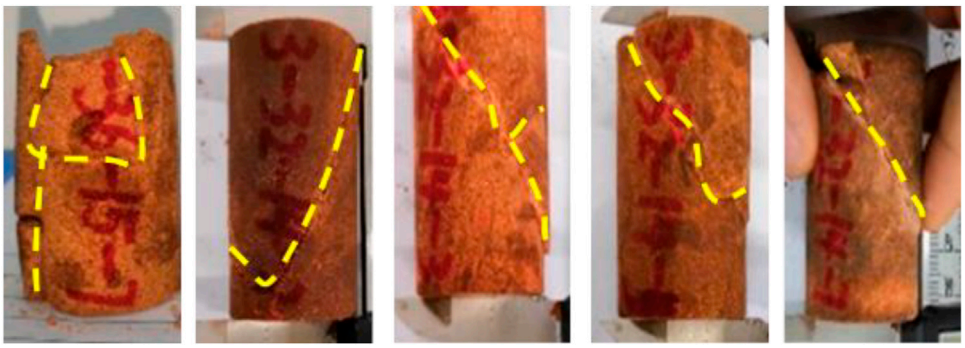

FIGURE 10 | The shape of sandstone specimens after failure in conventional triaxial compression.

FIGURE 11 | Three-axis failure modes of sandstone at different temperatures (25, 30, 60, 75, 90°C).

the nonlinear deformation is obvious in the initial test, but it diminishes gradually with the increase of confining pressure. And the sandstone changes from brittle to ductile failure under confining pressure. The variation trend of stress-strain curves of sandstone samples under different confining pressures is roughly the same, which can be divided into four stages: compaction, elasticity, yield and failure. In the compaction stage, the stress-strain curve is concave upward. The strain of sandstone decreases with the increase of stress, and the micro-fissure in sandstone closes under the action of external force. In this test, the sandstone particles are finer, and the binding force between the particles with smaller internal pores is weak, which can quickly be compacted under the action of external force. Therefore, the depression in the stress-strain curve during the compaction stage is not obvious. In the elastic stage, the stress-strain curve is linear, showing the elastic characteristics of sandstone. In the yielding stage, the sandstone is gradually destroyed and new micro-cracks are generated at the same time. With the continuous application of compressive stress, the micro-cracks continue to develop and expand, and develop into macro-cracks. Then going to the failure stage, the sandstone reaches its ultimate bearing capacity, and many macroscopic cracks penetrate the entire specimen. At last, the specimen gradually loses its bearing capacity, and the stress-strain curve shows a downward trend.

TABLE 3 | Sandstone damage rate at different temperatures.

Temperature *T*/C	Damage rate
25	0
30	0.26
60	0.51
75	0.57
90	0.61

The relationship between the maximum and minimum principal stresses of the peak stress state under different confining pressure conditions is shown in **Figure 5**. In the absence of confining pressure, the peak strength of sandstone is only 5.55 MPa. As the confining pressure increases, the peak strength of sandstone increases from 5.55 to 92.49 MPa. When the confining pressure is 20 MPa, 30 MPa, and 45 MPa, the peak strength of sandstone is increased by 75.14, 151.44, and 233.74%, respectively, compared with 27.71 MPa when the confining pressure is 10 MPa. **Figure 6** shows the changing trend of elastic modulus under the changing state of confining pressure. The results show that the elastic modulus of sandstone is positively correlated with the confining pressure.

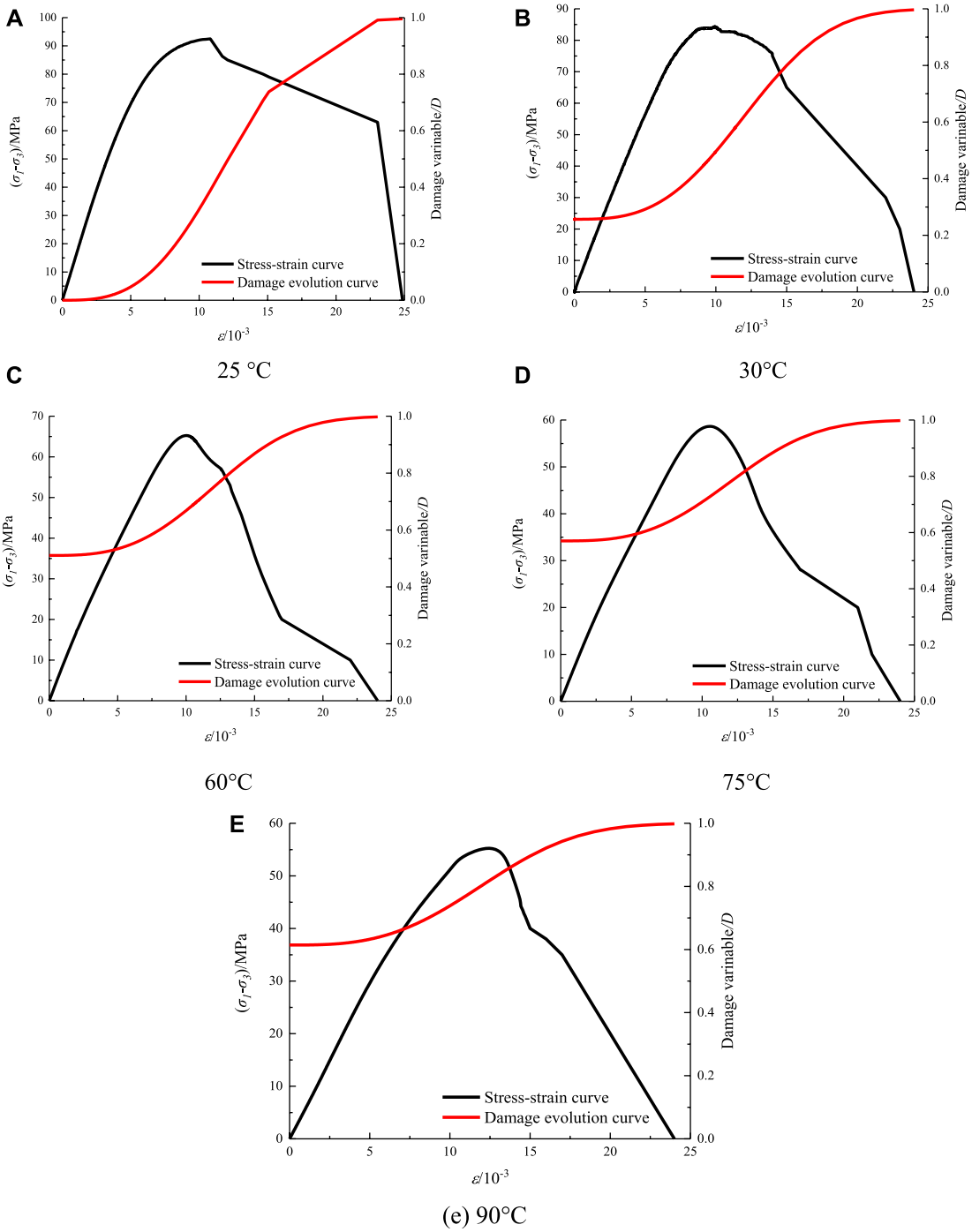

FIGURE 12 | Sandstone damage at different temperatures under 45 MPa confining pressure.

Analysis of Triaxial Compression Test Results at Different Temperatures

Figure 7 shows the stress-strain curves of sandstone at different temperatures (25°C, 30°C, 60°C, 75°C, 92°C) under confining pressure of 45 MPa. It can be seen from **Figure 7** that under the triaxial tests at different temperatures, sandstone undergoes a compaction stage (I), an elastic stage (II), a plastic deformation stage (III), a ductile failure stage (IV), and an instability failure stage (V). The changing trend of sandstone compaction stage and elastic stage under the triaxial tests at different temperatures is the same as that under conventional triaxial compression. In the plastic deformation stage, as the stress increases, the curve deviates from the square shape to produce irreversible plastic

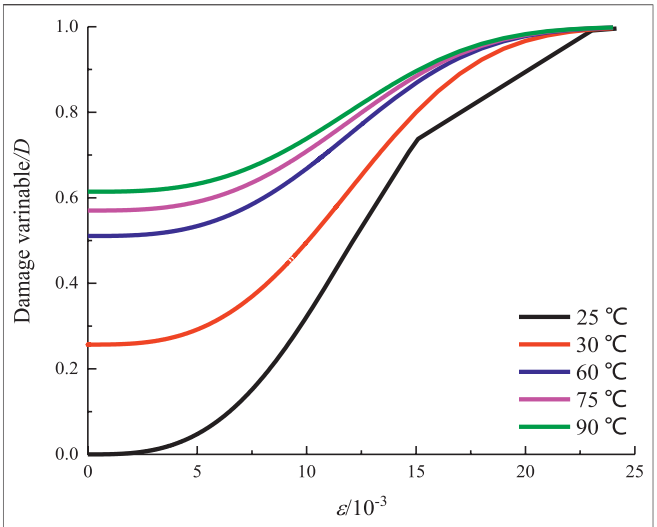

FIGURE 13 | thermal-mechanical coupling sandstone damage.

deformation, and the stress gradually reaches its peak strength. After the sandstone reaches its peak strength, it enters the ductile failure stage. The stress remains almost constant, but the strain continues to increase during the ductile failure stage. The higher the temperature, the more obvious the ductility stage, the more stable the stress level, and the gradual expansion of the cracks. In the instability failure stage, the sandstone loses its bearing capacity and undergoes brittle failure, and the failure mode of the sandstone under different temperatures is also different.

Table 2 shows the statistical values of mechanical parameters such as the peak strength of sandstone under triaxial compression at different temperatures and the same confining pressure.

Figure 8 shows the peak strength of sandstone as a function of temperature. It can be seen from **Figure 8** that as the temperature increases, the peak strength of sandstone decreases from 92.49 MPa at a temperature of 25°C–55.25 MPa. When the temperature increased from 30 to 60°C, the peak strength of sandstone dropped the most from 84.35 to 65.24 MPa. However, under the three gradient conditions of 60°C, 75°C, and 92°C, the peak strength decrease is relatively small. After curve fitting, the temperature and the peak strength meet the power function relationship, showing a negative correlation. As the temperature increases, the peak strength of the sandstone is attenuated. When the temperature exceeds 60°C, the attenuation rate gradually slows down.

Figure 9 shows the relationship between the elastic modulus of sandstone and the Poisson's ratio at different temperatures. As is shown in **Figure 9**, the elastic modulus of sandstone is 14.10 GPa at the temperature of 25°C (indoor temperature) and the confining pressure of 45 MPa. As the temperature increases, the elastic modulus decreases from 14.10 to 5.44 GPa. Compared with the elastic modulus under normal temperature conditions, the elastic modulus at high temperature decreases by 25.67, 51.06, 57.02, and 61.42%, respectively. The elasticity modulus is positively correlated with the temperature as an exponential function, and the Poisson's ratio is also an exponential function of temperature, but it increases with the increase of temperature.

Analysis of Failure Characteristics of Triaxial Compression

Figure 10 and **Figure 11** show the shape of the specimen after failure under different confining pressures and the triaxial failure mode of sandstone under different temperatures and different confining pressures. It can be seen from **Figure 10** that under low confining pressure (0 MPa, 10 MPa), the specimen shows shear failure and cracks penetrate the entire specimen. Under the action of high confining pressure (20 MPa, 30 MPa, 45 MPa), the specimen still shows shear failure (local shear failure), but the penetration length of the shear surface becomes shorter and shorter as the confining pressure increases. It is because the high confining pressure has a restraining effect on the test piece, which resists the damage of the test piece, and the test piece starts to fail from the weak structural surface.

According to the triaxial failure mode of sandstone at different temperatures, as shown in **Figure 11**, it can be seen that the triaxial compression of sandstone exhibits local shear failure at indoor temperatures. At 30°C, the sandstone suffered combined shear and tension failure, forming an irregularly shaped through the crack and some short cracks at the ends. At 60°C, a through crack appears in the sandstone but the radial depth is relatively shallow, which is also a combination of shear and tension failure. Because the specimen itself has a naturally weak structural surface, it fails along the weak structural surface under the axial action. Under the action of 75 and 90°C, the sandstone suffered from bulging failure without obvious damage and cracks, and some slagging phenomenon appeared at the end of the sandstone. When the sample was removed after the 90°C test, a section of the sample was missing due to human factors. But it can still be seen that the particle shedding of the specimen is more serious. Under the action of temperature, the cementation between particles is reduced, and the combined action of temperature and confining pressure also increases the ductility of sandstone.

SANDSTONE THERMAL-MECHANICAL DAMAGE EVOLUTION

When the material is subjected to an external load, cracks are formed along with the defects of the material itself. With the continuous application of the load, the continuous accumulation of micro-cracks and voids in the material leads to the gradual deterioration or damage of the material. The Weibull distribution is used to represent the statistical distribution law of the strength of the rock element body (Wu and Zhang 1996) namely:

$$F(\varepsilon) = \frac{m}{\alpha}\left(\frac{\varepsilon}{\alpha}\right)^{m-1} e^{-\left(\frac{\varepsilon}{\alpha}\right)^{m}} \quad (1)$$

Where: $F(\varepsilon)$ is the corresponding strength probability of the primitive body under micro-strain, ε is the micro-strain of the primitive body, α and m are the Weibull statistical distribution parameters.

Under the action of the triaxial compression, cracks are produced in sandstone under the action of stress, and cracks are gradually connected with the increase of stress, and the deformation and failure process can be regarded as continuous failure. The damage variable D_t is a description of the damage degree of the sandstone during the stress process, which can be expressed as:

$$D_t = \int_0^{\varepsilon} F(\varepsilon)d\varepsilon = 1 - \exp\left[-\left(\frac{\varepsilon}{\alpha}\right)^m\right] \quad (2)$$

According to the theory of macroscopic damage mechanics, the temperature damage to the rock can be characterized by the change of rock mechanics parameters, and the thermal damage variable (Liu and Xu, 2000) is defined as:

$$D_T = 1 - \frac{E_T}{E_0} \quad (3)$$

n the formula: E_0, E_T are the elastic modulus of the rock at indoor temperature (initial state) and different temperatures (thermal damage state), respectively. After calculation, the thermal damage at different temperatures is shown in the following **Table 3**:

Assuming that the temperature is at the indoor temperature, the sandstone has no thermal damage. According to **Table 3**, the thermal damage of sandstone gradually increases with the increase in temperature. The thermal damage evolution equation can be obtained by fitting the power function to the above thermal damage:

$$D_T = 0.1517^*(T-25)^{0.3369} \quad (4)$$

Under triaxial compression $\sigma_2 = \sigma_3$, according to the J. Lemaitre strain equivalence hypothesis (Lemaitre, 1984.; Zhang et al., 2014), the damage constitutive relationship of sandstone is as follows:

$$\sigma_1 = E\varepsilon_1(1-D) + 2\nu\sigma_3 \quad (5)$$

In the formula: E is the material elastic modulus matrix, ε_1 is the axial strain, ν is the Poisson's ratio. However, under the combined action of temperature and load, the damage to sandstone has multiple couplings, showing different damage characteristics. Substituting 2) and 4) into 5) to sort out, **eqn. 6**:

$$\sigma_1 = E_0[1 - a^*(T-b)^c]^* \exp\left[-\left(\frac{\varepsilon_1}{\alpha}\right)^m\right]^*\varepsilon_1 + 2\nu\sigma_3 \quad (6)$$

Eqn. 6 expresses the statistical constitutive relationship of sandstone damage under the coupling effect of constant confining pressure, triaxial compression, and temperature. In the formula: a is the material parameter, b is the initial temperature of thermal damage, and c is the slope of the tangent to the arc of the power function. The greater of c, greater the slope, that is, the faster the damage rate. α and m are the Weibull statistical distribution parameters, which are the same as **eqn. 1**.

According to **Eqn. 6**, the sandstone damage evolution under different temperatures of 45 MPa confining pressure is analyzed. **Figures 12A–E** shows the amount of sandstone damage at 45 MPa confining pressure at different temperatures. It can be seen from **Figure 12** that the damage degree of sandstone increases with the increase of strain. In the compaction stage, the damage is extremely small, almost close to zero. In the elastic stage, the damage degree of sandstone increases relatively slowly, because the elastic strain of sandstone itself resists the action of external load. However, as the external load increases, the plastic deformation of sandstone is gradually obvious, and the amount of damage is gradually increasing. At the same time, the original micro-cracks of sandstone gradually expand and produce new cracks, which make the sandstone specimen appear the cohesive macro cracks and lose stability in the finals.

Figure 13 shows the amount of sandstone damage under load and different temperatures. It can be seen from **Figure 13** that the sandstone has not been loaded at the indoor temperature or has not been damaged at the initial stage of loading. However, under the action of 30, 60, 75, and 90°C, a certain amount of damage has occurred to the sandstone when it is not loaded or at the initial stage of loading. This is because the sandstone is heated to the preset temperature during the test and kept at a constant temperature for 2 h. As the temperature increases, the initial damage to the sandstone is greater, and the damage amount is 0.25 at 30°C and 0.51 at 60°C. The obvious temperature difference and the difference in damage degree are also significant. But with the increase of strain, the difference in damage amount gradually decreases. This reason is the damage of particle slip and cracks caused by mechanical force is much greater than that caused by thermal expansion.

According to the sandstone test results and damage evolution analysis, it is shown that the temperature also causes the strong attenuation of the sandstone itself. The temperature intensifies the evaporation of the combined water in the minerals in the rock, leading to a decrease in the lubrication effects but an enhancement in the bonding strength and frictional force (Yin et al., 2021). And the crystalline structure or composition of some minerals in the sandstone is destroyed to a certain degree, which result the mechanical properties of weak layers of sandstone are affected. The temperature also accelerates the uneven expansion of different mineral particles in the rock, resulting in thermal stress inside the rock and irreversible thermal damage, which in combination with the mechanical stress causes cracks propagate rapidly, leading to an obvious increase in porosity and sharp degradation in the compression strength. The movement and deformation of sandstone particles caused by temperature accelerate the infiltration of original fractures and the formation of new fractures in the rock and eventually lead to the loss of bearing capacity of sandstone. However, with a continuous increase in the temperature, the thermal damage of

sandstone is enhanced and plays the principal role, resulting in a decrease in the compression strength.

CONCLUSION

Based on the triaxial compression and high-temperature triaxial compression tests of sandstone in gas storage, this paper studies the mechanical properties and thermal damage evolution process of sandstone under temperature and draws the following conclusions.

1) In the process of triaxial compression at indoor temperature, sandstone failure has undergone four stages, compaction stage, elastic stage, yield stage, and failure. Under the action of temperature, sandstone failure has undergone five stages: compaction stage, elastic stage, plastic deformation stage, ductile failure stage, and instability failure stage.
2) Under conventional triaxial compression, when the confining pressure rises from 10 to 45 MPa, the peak strength of sandstone increases by 233.74%. When the temperature increased from 25 to 90°C, the peak strength of sandstone with a confining pressure of 45 MPa dropped by 40.26%. In addition to the impact on the peak strength, the elastic modulus of sandstone also decreases with increasing temperature, while Poisson's ratio gradually increases. Confining pressure and temperature can reduce the brittleness of sandstone and increase ductility.
3) Established the damage constitutive relationship of gas storage sandstone under the coupling effect of triaxial compression and temperature. At different temperatures, the damage degree of sandstone gradually increases with the increase of strain. When the peak strain is exceeded, the damage growth rate gradually increases. The particles in the sandstone are expanded and the thermal movement of the particles accelerates under the action of temperature, which accelerates the expansion of the micro-cracks. Therefore, the damage degree of the sandstone gradually increases with the increase in temperature.

DATA AVAILABILITY STATEMENT

The original contributions presented in the study are included in the article/Supplementary Material, further inquiries can be directed to the corresponding author.

AUTHOR CONTRIBUTIONS

BYZ conceived and designed the research method, theoretical research and paper revision. XPW and LHW completed the damage model, data analysis, and the writing of the paper manuscript. XPW and YJW completed the experiment. JSY and JCS provided sandstone samples and economically supported the project.

FUNDING

This work was supported by The National Natural Science Foundation of China (Grant No.41302223, 51809151), The Science and Technology Research Program of Chongqing Municipal Education Commission (Grant No. KJZD-K202101505), The Natural Science Foundation of Chongqing (No. cstc2020jcyj-msxm1078, No. cstc2020jcyj-msxmX0558, No.cstc2020jcyj-msxmX0567), The Open Fund for Key Laboratory of Reservoir Dam Safety of Ministry of Water Resources of China (YK321012), The Innovative group project of Natural Science Foundation of Hubei Province (2020CFA049), Chongqing University of Science and Technology Graduate Students' Science and Technology Innovation Program (YKJCX2020653).

REFERENCES

Beibei Yang, B., He, M., and Chen, Y. (2020). Experimental Study of Nonlinear Damping Characteristics on Granite and Red Sandstone under the Multi-Level Cyclic Loading-Unloading Triaxial Compression. *Arab. J. Geosci.* 13, 72. doi:10.1007/s12517-019-5022-8

Chen, Y., Zuo, J., Liu, D., Li, Y., and Wang, Z. (2021). Experimental and Numerical Study of Coal-Rock Bimaterial Composite Bodies Under Triaxial Compression. *Int. J. Coal Sci. Technol.* 8 (5), 908–924. doi:10.1007/s40789-021-00409-5

Corfdir, A., and Sulem, J. (2008). Comparison of Extension and Compression Triaxial Tests for Dense Sand and Sandstone. *Acta Geotech.* 3 (3), 241–246. doi:10.1007/s11440-008-0068-x

Kumari, W. G. P., Beaumont, D. M., Ranjith, P. G., Perera, M. S. A., Avanthi Isaka, B. L., and Khandelwal, M. (2019). An Experimental Study on Tensile Characteristics of Granite Rocks Exposed to Different High-Temperature Treatments. *Geomech. Geophys. Geo-energ. Geo-resour.* 5 (1), 47–64. doi:10.1007/s40948-018-0098-2

Lemaitre, J. (1984). How to Use Damage Mechanics. *Nucl. Eng. Des.* 80 (2), 233–245. doi:10.1016/0029-5493(84)90169-9

Li, L., and Gong, F. (2020). Experimental Investigation on the Energy Storage Characteristics of Red Sandstone in Triaxial Compression Tests with Constant Confining Pressure. *Shock Vib.* 2020, 1–11. doi:10.1155/2020/8839761

Liu, Q. S., and Xu, X. C. (2000). Damage Analysis of Brittle Rock under Temperature. *Chin. J. Rock Mech. Eng.* 19 (04), 408–411.

Ma, X., Wang, G., Hu, D., Liu, Y., Zhou, H., and Liu, F. (2020). Mechanical Properties of Granite under Real-Time High Temperature and Three-Dimensional Stress. *Int. J. Rock Mech. Min. Sci.* 136, 104521. doi:10.1016/j.ijrmms.2020.104521

Meng, Q.-b., Qian, W., Liu, J.-f., Zhang, M.-w., Lu, M.-m., and Wu, Y. (2020). Analysis of Triaxial Compression Deformation and Strength Characteristics of Limestone after High Temperature. *Arab. J. Geosci.* 13 (4), 1–14. doi:10.1007/s12517-020-5151-0

Meng, Q.-b., Liu, J.-F., Pu, H., Yu, L.-y., Wu, J.-y., and Wang, C.-k. (2021). Mechanical Properties of Limestone after High-Temperature Treatment under Triaxial Cyclic Loading and Unloading Conditions. *Rock Mech. Rock Eng.* 54 (12), 6413–6437. doi:10.1007/s00603-021-02638-1

Mohamadi, M., and Wan, R. G. (2016). Strength and Post-peak Response of Colorado Shale at High Pressure and Temperature. *Int. J. Rock Mech. Min. Sci.* 84, 34–46. doi:10.1016/j.ijrmms.2015.12.012

Qian, Q. H. (2007). "The Characteristic Scientific Phenomenon of Deep Rock Mass Engineering Response and the Definition of "deep"," in *The Selected Papers of Academician Qian Qihu* (Beijing, China: Chinese Society of Rock Mechanics and Engineering).

Qin, Y., Tian, H., Xu, N.-X., and Chen, Y. (2020). Physical and Mechanical Properties of Granite after High-Temperature Treatment. *Rock Mech. Rock Eng.* 53 (1), 305–322. doi:10.1007/s00603-019-01919-0

Sheng-Qi Yang, S.-Q., Tian, W.-L., Elsworth, D., Wang, J.-G., and Fan, L.-F. (2020). An Experimental Study of Effect of High Temperature on the Permeability Evolution and Failure Response of Granite under Triaxial Compression. *Rock Mech. Rock Eng.* 53 (10), 4403–4427. doi:10.1007/s00603-019-01982-7

Taheri, S. R., Pak, A., Shad, S., Mehrgini, B., and Razifar, M. (2020). Investigation of Rock Salt Layer Creep and its Effects on Casing Collapse. *Int. J. Min. Sci. Technol.* 30 (3), 357–365. doi:10.1016/j.ijmst.2020.02.001

Tang, Z. C., Sun, M., and Peng, J. (2019). Influence of High Temperature Duration on Physical, Thermal and Mechanical Properties of a Fine-Grained Marble. *Appl. Therm. Eng.* 156, 34–50. doi:10.1016/j.applthermaleng.2019.04.039

Wang, G., Yang, D., Zhao, Y., Kang, Z., Zhao, J., and Huang, X. (2019). Experimental Investigation on Anisotropic Permeability and its Relationship with Anisotropic Thermal Cracking of Oil Shale under High Temperature and Triaxial Stress. *Appl. Therm. Eng.* 146, 718–725. doi:10.1016/j.applthermaleng.2018.10.005

Wang, J., Zhang, Q., Song, Z., and Zhang, Y. (2020). Creep Properties and Damage Constitutive Model of Salt Rock Under Uniaxial Compression. *Int. J. Damage Mech.* 29 (6), 902–922. doi:10.1177/1056789519891768

Wang, J., Zhang, Q., Song, Z., Liu, X., Wang, X., and Zhang, Y. (2022). Microstructural Variations and Damage Evolvement of Salt Rock Under Cyclic Loading. *Int. J. Rock Mech. Min. Sci. Geomech. Abstr.* 152, 105078. doi:10.1016/j.ijrmms.2022.105078

Wu, Z., and Zhang, C. J. (1996). Research on Rock Damage Model and its Mechanical Characteristics under Unidirectional Load. *Chin. J. Rock Mech. Eng.* 15 (01), 55–61.

Xiao, F., Jiang, D., Wu, F., Zou, Q., Chen, J., Chen, B., et al. (2021). Effects of High Temperature on the Mechanical Behaviors of Sandstone under True-Triaxial Unloading Conditions. *Bull. Eng. Geol. Environ.* 80 (6), 4587–4601. doi:10.1007/s10064-021-02205-6

Xie, H. P. (2017). *Deep Rock Mass Mechanics And Mining Theory* Research Concept and Expected Results. *Eng. Sci. Technol.* 49 (02), 1–16. doi:10.15961/j.jsuese.201700025

Yin, Q., Wu, J., Zhu, C., He, M., Meng, Q., and Jing, H. (2021). Shear Mechanical Responses of Sandstone Exposed to High Temperature under Constant Normal Stiffness Boundary Conditions. *Geomech. Geophys. Geo-energ. Geo-resour.* 7 (2), 1–17. doi:10.1007/s40948-021-00234-9

Zhang, H. M., Lei, L. N., and Yang, G. S. (2014). Rock Damage Model under Temperature and Load. *Chin. J. Rock Mech. Eng.* 33 (S2), 3391–3396. doi:10.13722/j.cnki.jrme.2014.s2.001

Zhang, W., Sun, Q., Zhu, Y., and Guo, W. (2019). Experimental Study on Response Characteristics of Micro-macroscopic Performance of Red Sandstone after High-Temperature Treatment. *J. Therm. Anal. Calorim.* 136, 1935–1945. doi:10.1007/s10973-018-7880-9

Zhao, Y. S., Wan, Z. J., Feng, Z. J., Xu, Z. H., and Liang, W. G. (2017). Evolution of Mechanical Properties of Granite at High Temperature and High Pressure. *Geomech. Geophys. Geo-energ. Geo-resour.* 3 (2), 199–210. doi:10.1007/s40948-017-0052-8

Zhou, X.-P., Li, G.-Q., and Ma, H.-C. (2020). Real-time Experiment Investigations on the Coupled Thermomechanical and Cracking Behaviors in Granite Containing Three Pre-existing Fissures. *Eng. Fract. Mech.* 224, 106797. doi:10.1016/j.engfracmech.2019.106797

Zhou, X., Fu, L., Cheng, H., and Berto, F. (2021). Cracking Behaviours of Rock-like Materials Containing Three Preexisting Flaws after High-temperature Treatments. *Fatigue Fract. Eng. Mater Struct.* 44 (3), 622–635. doi:10.1111/ffe.13382

Zhou, X. P. (2006). Triaxial Compressive Behavior of Rock with Mesoscopic Heterogenous Behavior: Strain Energy Density Factor Approach. *Theor. Appl. Fract. Mech.* 45 (1), 46–63. doi:10.1016/j.tafmec.2005.11.002

Zhu, Z., Tian, H., Wang, R., Jiang, G., Dou, B., and Mei, G. (2021). Statistical Thermal Damage Constitutive Model of Rocks Based on Weibull Distribution. *Arab. J. Geosci.* 14 (6), 1–14. doi:10.1007/s12517-021-06730-2

Conflict of Interest: The author declares that, concerning the publication of this paper and the funding for publishing this paper, there is not any conflict of interest.